The Hexagonal Phase and Melt of Low Molecular Weight Polyethylene(Dissertation_全文)

AUTHOR(S):

Asahi, Takanao

学位申請論文

朝日孝尚

主論文

The Hexagonal Phase and Melt of Low Molecular Weight Polyethylene

Takanao Asahi

Department of Physics, Faculty of Science,
Kyoto University, Kyoto, Japan

Synopsis

Phase diagrams of low molecular weight polyethylene (M=1000, 2000, 6500, 16000) and polyethylene (M≈1000) after fuming nitric acid treatment are determined from 20°C to 300°C up to pressures of about 10 kbar. The fractions with molecular weight 1000 and 2000 do not exhibit the hexagonal phase, but the others do. Effects of molecular weight and fuming nitric acid treatment on the phase diagrams are discussed in terms of the entropy of the melt.

Introduction

The high-pressure hexagonal phase of polyethylene was discovered and studied by Bassett[1], and is the subject of a recent review[2]. The structure of this form has been clarified by X-ray diffraction[3,4] and Raman spectroscopy[5]; it has been found that many defects are involved in the crystal. The stability of such a disordered phase has also been discussed thermodynamically[6,7] and studied experimentally referring to the effects of cross linking[8]. Since this phase is closely related to the appearance of extended-chain crystals (ECC), it is important to study the effect of molecular weight on the stability of the hexagonal phase.

The hexagonal phase has been studied mainly in polyethylene with molecular weight greater than 1×10^4. The effect of molecular weight distribution on the phase transition was discussed by Hikosaka et al.[9,10] A study by Takamizawa et al.[11] is the only one which shows experimentally the effect of molecular weight on the phase diagram of polyethylene of relatively low molecular weight, although at that time the hexagonal phase had not been recognized. Their differential thermal analysis (DTA) at p=5 kbar can be interpreted as follows: 1) A lower limit of molecular weight exists for the hexagonal phase; it is greater than 6.5×10^3 and smaller than 1.3×10^4 at p=5 kbar. 2) As the molecular weight increases, the melting temperature of the hexagonal phase increases more rapidly than the transition temperature for the orthorhombic to hexagonal transition.

On the other hand, Yamamoto and Asai[12] showed that low

molecular weight polyethylene (M_n=1260) obtained by fuming nitric acid (FNA) treatment exhibited the high pressure phase. They ascribed this result to the change in the structure of lamellar surface caused by the FNA treatment.

Here we report phase diagrams of low molecular weight fractions and FNA-treated polyethylene up to 15 kbar. The structure of the high-pressure phase of FNA-treatred polyethylene is examined by X-ray diffraction. The effects of molecular weight and FNA treatment on the stability of the hexagonal phase are discussed in terms of the entropy of the melt of polyethylene of finite chain length.

Experimental

The materials used were four kinds of fractionated polyethylene and two kinds of FNA-treated polyethylene. Their characteristics are shown in Table 1.

M1000FNA was prepared as follows : melt crystallized M1000 was immersed in FNA at 70°C for 8 days. Since M1000 crystallized without folding, it was attacked by FNA only at the chain ends. Therefore, the molecular weight of M1000FNA is believed to be about 1000.

SholexFNA was prepared as follows: melt crystallized Sholex 6009 ($M_n=1.4\times10^4$, M_w/M_n=8.1) was drawn and immersed in FNA at 60°C for 4 days. In this case, chains were attacked at folds as well as chain ends. The long spacing determined by SAXS was 180A before FNA treatment, so that the molecular weight of SholexFNA is estimated as about 1300.

Phase diagrams of the materials except for SholexFNA were

determined by X-ray diffraction. A high-pressure cell of the diamond anvil type was used with a stainless-steel gasket 0.3 mm thick. The pressure transmitting fluid was water. The X-ray diffraction photographs were taken on flat films with MoKα radiation filtered by zirconium. Pressure was measured by the shift of the 002 reflection of graphite[3]. Coexistence of the orthorhombic phase and the hexagonal phase was ascertained by X-ray diffraction. Melting of the orthorhombic phase and the hexagonal phase was observed optically with a polarized microscope[3].

The structure of the hexagonal phase of FNA-treated polyethylene was studied on the oriented material, SholexFNA. X-ray fiber photographs were taken on flat films with MoKα radiation monochromatized by a graphite single crystal[3,4].

Infrared spectra were obtained on FNA-treated polyethylene dispersed in KBr pellets.

Results

1. Phase diagrams

Phase diagrams of the four kinds of fractionated polyethylene are shown in Fig. 1.

M1000 and M2000 do not show the hexagonal phase in the pressure range of the experiment. In particular, M2000 shows no hexagonal phase up to p=15 kbar. The melting temperature T^{m-0} of the orthorhombic M2000 is higher than that of M1000 by 14°C at each pressure. These phase diagrams agree well with those obtained by DTA measurement at pressures below 5 kbar[13].

M6500 and M16000 exhibit the hexagonal phase. The

transition temperatures for the orthorhombic to hexagonal transition, T^{h-o}, are almost the same for both specimens at each pressure. On the other hand, the melting temperature of the hexagonal phase, T^{m-h}, of M16000 is higher than that of M6500 by 10 or 15°C.

The phase diagram of M1000FNA is shown in Fig. 2. For comparison, the phase diagram of M1000 is also shown. There are two marked effects of FNA treatment. First, T^{m-o} of M1000-FNA is higher than that of M1000 by 10°C at atmospheric pressure[14]. Secondly M1000FNA exhibits a hexagonal phase at pressures above 4 kbar.

2. Structure of the hexagonal phase of FNA-treated polyethylene

X-ray fiber photographs of SholexFNA in the hexagonal phase are shown in Fig. 3. These photographs are essentially the same as those of nontreated polyethylene[3,4]; there are three Bragg reflections, 100, 110 and 200, on the equator, and diffuse scattering with no appreciable Bragg reflection off the equator. Positions and widths of the diffuse scattering of SholexFNA agree well with those of NBS standard polyethylene. This result shows that the degree of disorder in the hexagonal phase of FNA-treated polyethylene is comparable to that of non-treated polyethylene.

Discussion

1. Effect of molecular weight on the hexagonal phase

Figure 1 shows that the lower limit of molecular weight for which the hexagonal phase exists is greater than 2000 and

smaller than 6500 for $p \leq 15$ kbar. As molecular weight decreases the melting temperature of the hexagonal phase, T^{m-h}, decreases more rapidly than the transition temperature for the orthorhombic to hexagonal transition T^{h-o}. Eventually the hexagonal phase disappears within the pressure range of the experiments for M2000 and M1000.

Low molecular weight polyethylene crystallizes without folding under high pressure in this experiment. Therefore, the theory developed by Flory and Vrij[15] on melting of n-paraffin is applicable to this problem. The difference in molar Gibbs' free energy between the orthorhombic phase and the melt can be expressed as follows.

$$G^m - G^o = x \cdot \Delta G_\infty^{m-o} + \Delta G_e^{m-o} - RT \cdot \ln x \quad , \qquad (1)$$

where x is the carbon number of molecule, ΔG_∞^{m-o} is the free energy of fusion per CH_2 in the limit $x=\infty$ at the temperture T and ΔG_e^{m-o} is the end-group contribution assumed to be constant for all x. The most important term in the present case is the last term, RT ln x. It comes from the "unpairing of end groups"[15] of neighboring molecules upon melting; end groups can adjoin to any portion of other chains in the melt. Lattice theory of chain liquids also gives this term.

ΔG_∞^{m-o} is approximately given by:

$$\Delta G_\infty^{m-o}(T) = (T_\infty^{m-o} - T) \cdot \Delta S_\infty^{m-o} \quad , \qquad (2)$$

where ΔS_∞^{m-o} is the entropy of fusion at the limiting melting

temperature T_{∞}^{m-o}. Then we obtain the melting temperature T_x^{m-o} for a given carbon number x from eq.(1):

$$T_x^{m-o} = T_{\infty}^{m-o}\left(1 + \frac{\Delta G_e^{m-o}}{xT_{\infty}^{m-o}\cdot\Delta S_{\infty}^{m-o}}\right)\Big/\left(1 + \frac{R\cdot\ln x}{x\cdot\Delta S_{\infty}^{m-o}}\right)$$

$$\cong T_{\infty}^{m-o} - \frac{RT_{\infty}^{m-o}\cdot\ln x}{x\cdot\Delta S_{\infty}^{m-o}} + \frac{\Delta G_e^{m-o}}{x\cdot\Delta S_{\infty}^{m-o}} \quad , \qquad (3)$$

Similarly, the melting temperature of the hexagonal phase for finite chain length is given by the following equation.

$$T_x^{m-h} \cong T_{\infty}^{m-h} - \frac{RT_{\infty}^{m-h}\cdot\ln x}{x\cdot\Delta S_{\infty}^{m-h}} + \frac{\Delta G_e^{m-h}}{x\cdot\Delta S_{\infty}^{m-h}} \quad , \qquad (4)$$

where ΔS_{∞}^{m-h} is the entropy of melting at the limiting melting temperature T_{∞}^{m-h} and ΔG_e^{m-h} is the end-group contribution. On the other hand the transition temperature for the orthorhombic to hexagonal transition is given as follows.

$$T_x^{h-o} = T_{\infty}^{h-o} + \frac{\Delta G_e^{h-o}}{x\cdot\Delta S_{\infty}^{h-o}} \quad , \qquad (5)$$

because the "unpairing of end groups" does not occur in the solid state transition. The equations (3), (4) and (5) represent the effect of molecular weight on the transition tempertures for a given pressure.

Here we can check the applicability of eq.(3) to low molecular weight polyethylene. The results are shown in Table 2. In this calculation we used the following values for the several parameters : T_{∞}^{m-0}=415K[16], ΔS_{∞}^{m-0}=9.91 J/mol·K, and ΔG_e^{m-0}=-13.7 kJ/mol[17]. The agreement is satisfactory. It

should be noted that the second term, the effect of chain length on the entropy of the melt, is as important as the contribution of the end group to the free energy of the crystal. For eq.(4), the second term plays an essential contribution, since ΔS_∞^{m-h} is about one fourth of ΔS_∞^{m-0}: ΔS_∞^{m-h}=2.3 J/mol·K[18]. For M6500 and M16000, the values of the second term are 12K and 25K respectively; the difference, 13K, is comparable to the experimental value, 10 or 15K. This fact shows that the last term in eq.(4) can contribute at most a few degrees for M6500 and M16000. The last term in eq.(5) also contributes to T_x^{h-0} by a few degrees for M6500 and M16000 as shown in Fig. 1.

2. Effect of FNA treatment

FNA-treated polyethylene (M1000FNA) exhibits a hexagonal phase in spite of its low molecular weight. One of the most important chemical changes induced by FNA treatment is the replacement of end groups by -COOH, partly by $-NO_2$[19]. This chemical change is confirmed by the IR spectrum. Thus FNA-treated polyethylene is a dicarboxylic acid with a large number of carbon atoms. Carboxyl groups make strong hydrogen bonds; bond energy is about 7 kcal/mol[20]. Molecules in the melt are joined by hydrogen bonds along the chain axis; they behave as a chain of high molecular weight. The second terms of eq.(3) and (4) will become very small due to effectively large x for FNA-treated polyethylene: dicarboxylic acids. Thus T^{m-0} and T^{m-h} are raised. Although the twisting of chain to make hydrogen bonds and dipole-dipole interaction must be taken into account in terms of ΔG_e^{m-h} and ΔG_e^{m-0}, the decrease

in the entropy of the melt is essentially responsible for the appearance of the hexagonal phase.

In fact a dicarboxylic acid of very low molecular weight, 1, 20-Eicosanedioic Acid, $HOOC(CH_2)_{18}COOH$, has been found to exhibit a high pressure phase (Fig. 4). At atmospheric pressure, it has a monoclinic crystal structure and melts directly without phase transition. But a solid-solid phase transition was observed at p=5.8 kbar, T=201°C and p=6.8 kbar, T=215°C. The high pressure phase is similar to the hexagonal phase of polyethylene. Only one Bragg reflection is strong, which corresponds to the side packing of chains. Bragg reflections corresponding to the periodicity along the chain direction is not observed in the high pressure phase. This fact implies disorder along the chain axis.

Melting temperatures of the dicarboxylic acid homologs are almost constant at about 125°C for even carbon numbers from 14 to 34[21]. These homologs will certainly have a high-pressure phase. Experiments on them, now progressing in our laboratory, will help us to understand the high-pressure phase of polyethylene.

Conclusion

As discussed above, the entropy of the melt plays an important role in explaining the effects of molecular weight and FNA treatment on the stability of the hexagonal phase.

It was reported that cross linking of polyethylene makes the triple point decrease markedly; even at atmospheric pressure, the hexagonal phase can appear[8]. Constrained fibers

from stirring crystallization of solution also shows hexagonal phase at atmospheric pressure[22]. Both of these phenomena can be easily described by the decrease of entropy in the molten state[8,22]. On cross linking, chain configuration is restricted. The constrained fiber is also restricted in the elongated state even after melting. Therefore, a decrease in the entropy of the melt composed of the "long molecular chains" is the essential factor for the appearance of the hexagonal phase.

Acknowledgments

The auther wishes to express his gratitude to Professor K. Asai and to Dr. H. Miyaji of Kyoto University for valuable discussions and encouragement throughout this work. He also wishes to thank Dr. S. Hosomi (Idemitsu Sekiyukagaku Co., Ltd.) for supplying the fractionated polyethylenes M6500 M16000.

References

1. D. C. Bassett, S. Block and G. J. Piermarini, J. Appl. Phys., 45, 4146 (1974).
2. D. C. Bassett, in Developments in Crystalline Polymers -1, D. C. Bassett ED., Applied Science Publishers Ltd., Essex, England, 1982, pp. 115-150.
3. T. Yamamoto, H. Miyaji and K. Asai, Jpn. J. Appl. Phys., 16, 1891 (1977).
4. T. Yamamoto, J. Macromol. Sci. Phys., B16, 487 (1979).
5. S. L. Wunder, Macromolecules, 14, 1024 (1981).
6. D. C. Bassett and B. Turner, Phil. Mag., 29, 925 (1974).
7. K. Asai, Polymer, 23, 391 (1982).
8. G. Ungar and A. Keller, Polymer, 21, 1273 (1980).
9. M. Hikosaka, S. Minomura and T. Seto, Jpn. J. Appl. Phys., 19, 1763 (1980).
10. M. Hikosaka, Jpn. J. Appl. Phys., 20, 617 (1981).
11. K. Takamizawa, Y. Urabe, A. Ohno and T. Takemura, Polymer Preprints, Japan, 22, 447 (1973).
12. T. Yamamoto and K. Asai, Polymer Preprints, Japan, 27, 1828 (1978).
13. K. Takamizawa, Y. Sasaki, K. Kono and Y. Urabe, Rep. Prog. Polym. Phys. Japan, 19, 285 (1976).
14. A. Keller and Y. Udagawa, J. Polym. Sci., A-2, 8, 19 (1970).
15. P. J. Flory and A. Vrij, J. Am. Chem. Soc., 85, 3548 (1963).

16. B. Wunderlich, Macromolecular Physics, vol. 3, Academic Press, London, 1980, Chap. 8.

17. C. M. L. Atkinson and M. J. Richardson, Trans. Faraday Soc., 65, 1749 (1969).

18. T. Ide, S. Taki and T. Takemura, Jpn. J. Appl. Phys., 16, 647 (1977).

19. R. P. Palmer and A. J. Cobbold,, Makromol. Chem., 74, 174 (1964).

20. G. C. Pimentel and A. L. McClellan, The Hydrogen Bond, W. H. Freeman and Company, San Francisco, 1960.

21. P. J. Housty and M. Hospital, Acta. Cryst., 21, 553 (1966).

22. A. J. Pennings and A. Zwijnenburg, J. Polym. Sci. Polym. Phys. Ed., 17, 1011 (1979).

Table 1 Characteristics of Each Sample: Molecular Weight, the Ratio of Weight to Number-Averaged Molecular Weight and Melting Temperature at p=1 atm.

Sample	M	M_w/M_n	T^{m-0} (K)
M1000	1000	1.1	379
M2000	2000	1.1	395
M6500	6500	1.14	407
M16000	16000	1.18	410
M1000FNA	∿1000	——	389
SholexFNA	∿1300	——	398

Table 2 Calculated Values of the Terms in eq.(3) and Comparison with Experimental Values

M	x	$\frac{RT_{\infty}^{m-o} \ln x}{x \cdot \Delta S_{\infty}^{m-o}}$	$-\frac{\Delta G_{e}^{m-o}}{x \cdot \Delta S_{\infty}^{m-o}}$	$\Delta T_{calc.}$ *	$\Delta T_{exp.}$ **
1000	71	20.9	19.5	40.4	36
2000	143	12.1	9.7	21.8	20
6500	464	4.6	3.0	7.6	7
16000	1143	2.1	1.2	3.3	4

* $\Delta T_{calc.} = (T_{\infty}^{m-o} - T_{x}^{m-o})_{calc.}$

** $\Delta T_{exp.} = (T_{\infty}^{m-o} - T_{x}^{m-o})_{exp.}$

Figure Captions

Figure 1. Phase diagrams of fractionated polyethylene, M1000, M2000, M6500 and M16000: h-m, hexagonal to melt transition; o-h, orthorhombic to hexagonal transition; o-m, orthorhombic to melt transition.

Figure 2. Phase diagrams of fuming nitric acid treated polyethylene M1000FNA and M1000.

Figure 3. X-ray fiber photographs of SholexFNA in the hexagonal phase (∿8 kbar, 265°C): (a) fiber axis is perpendicular to the incident beam, (b) fiber axis is tilted 16°C from the perpendicular position to the incident beam to permit the 002 reciprocal lattice point to intersect Ewald's sphere.

Figure 4. X-ray photographs of 1, 20 Eicosanedioic Acid: (a) in the monoclinic phase (6.2 kbar, 199°C), (b) in the coexisting state of the monoclinic and the high pressure phase (6.8 kbar, 215°C), (c) in the high pressure pnase (8.3 kbar, 229°C). The outer most rings are 002 reflection of graphite.

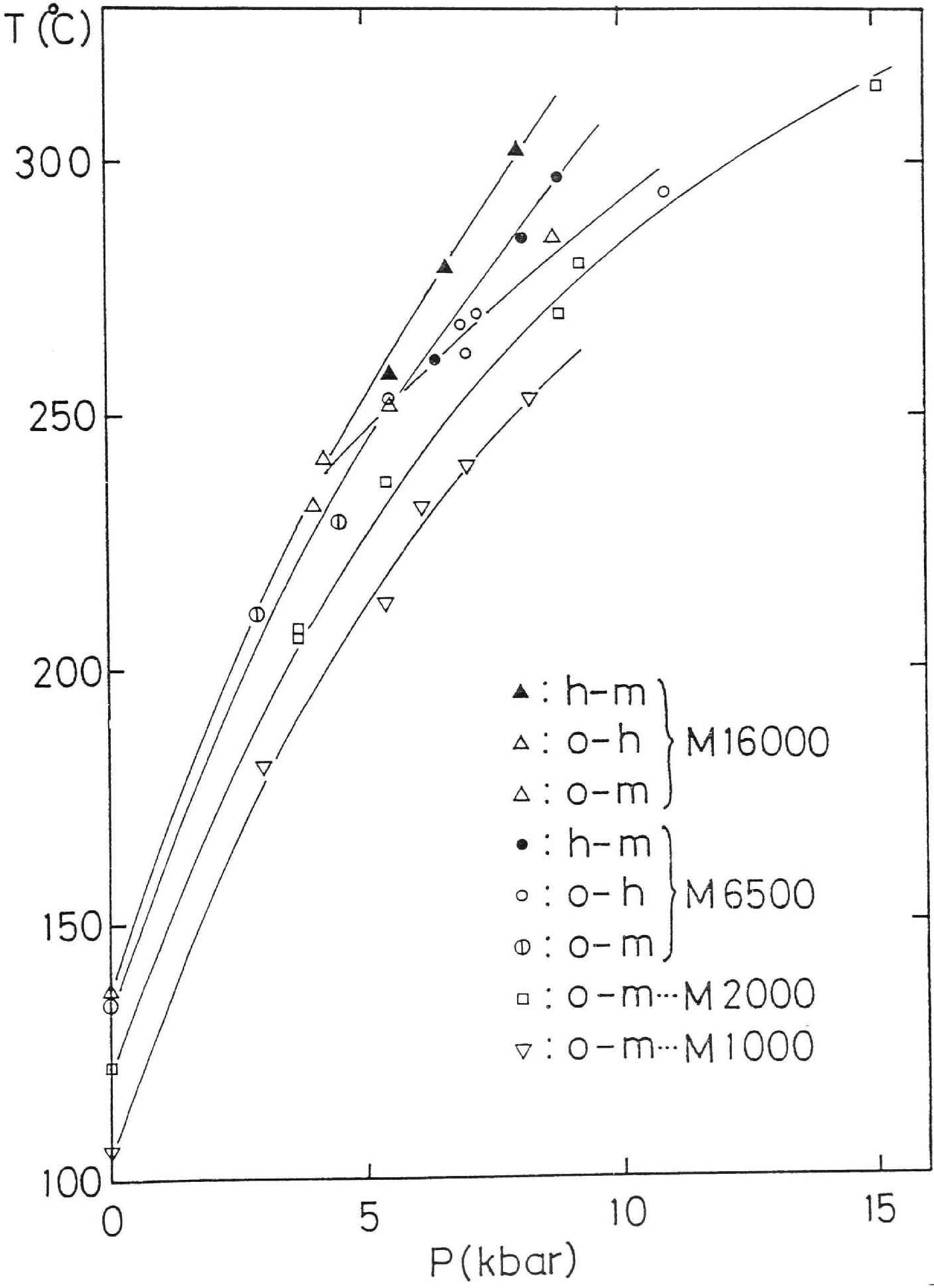
T (°C)
300
250
200
150
100
0
5
10
15
P(kbar)
▲ : h-m
△ : o-h
△ : o-m
M16000
● : h-m
○ : o-h
⊖ : o-m
M6500
□ : o-m…M2000
▽ : o-m…M1000

Fig. 1

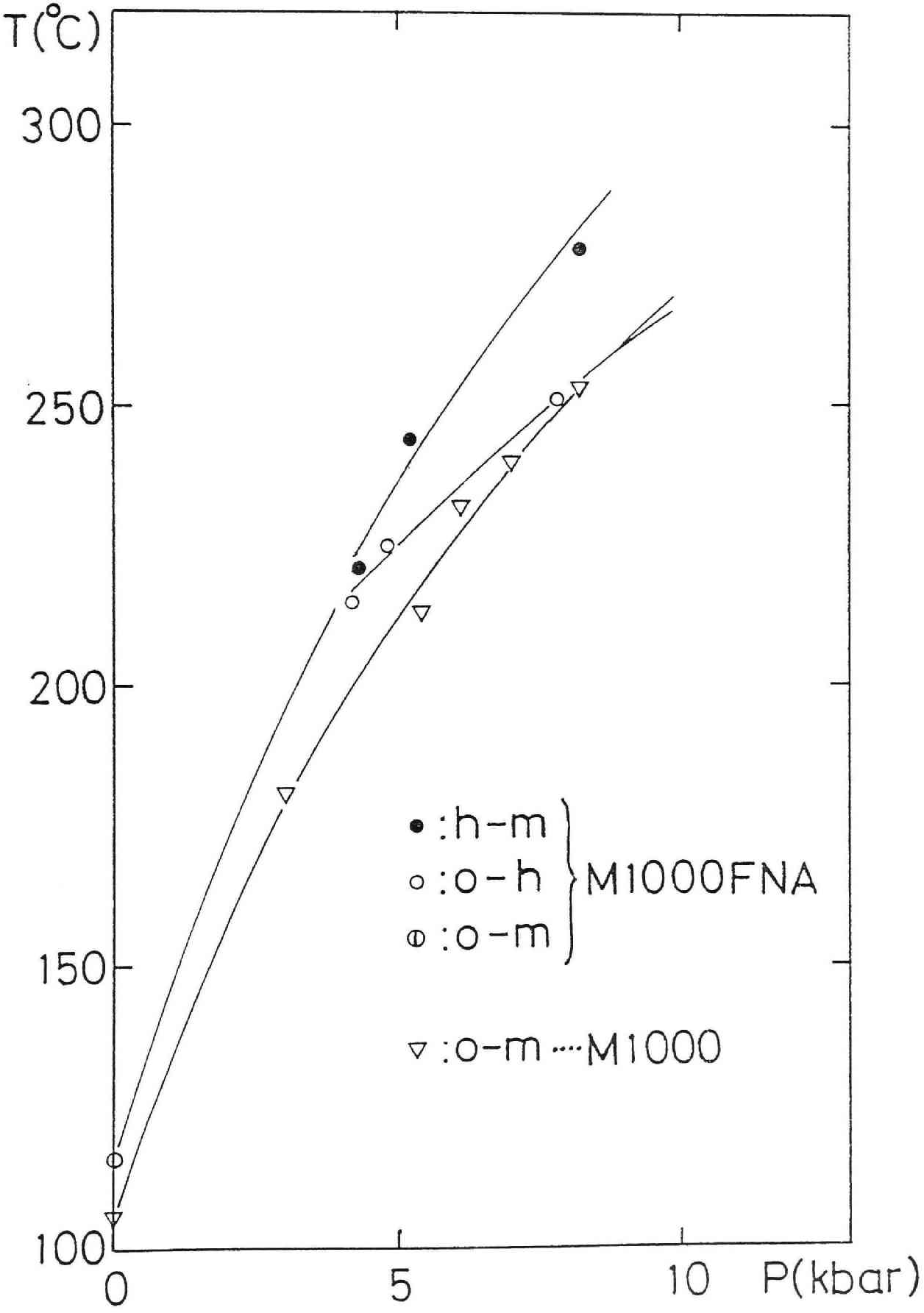
T(°C)
300
250
200
150
100
0
5
10
P(kbar)
●:h-m
○:o-h
⊕:o-m
M1000FNA
▽:o-m ····M1000

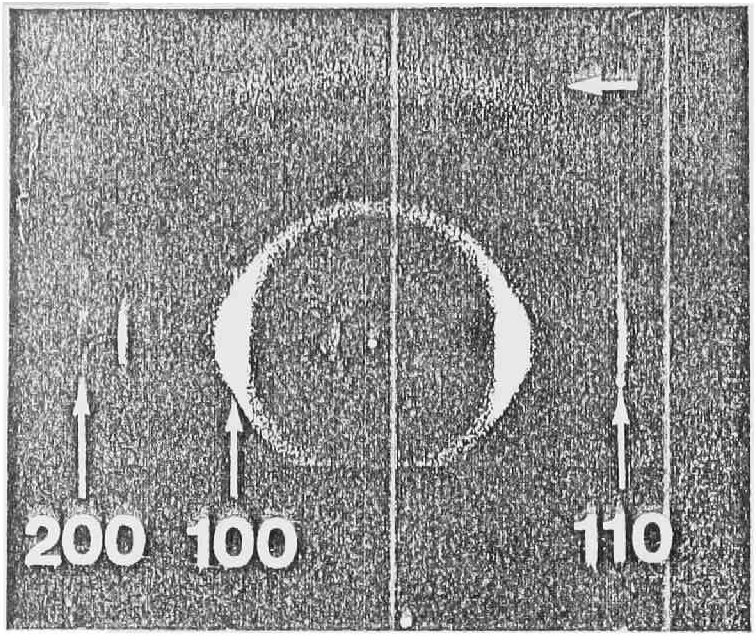
200
100
110

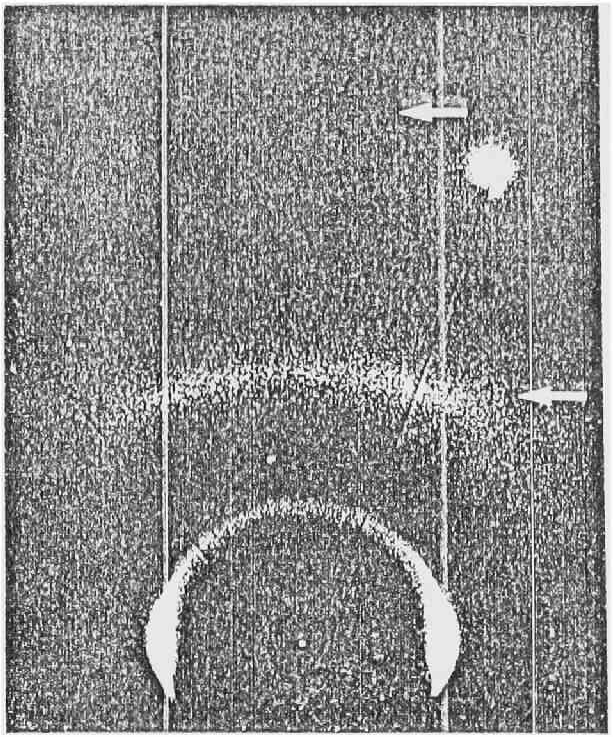

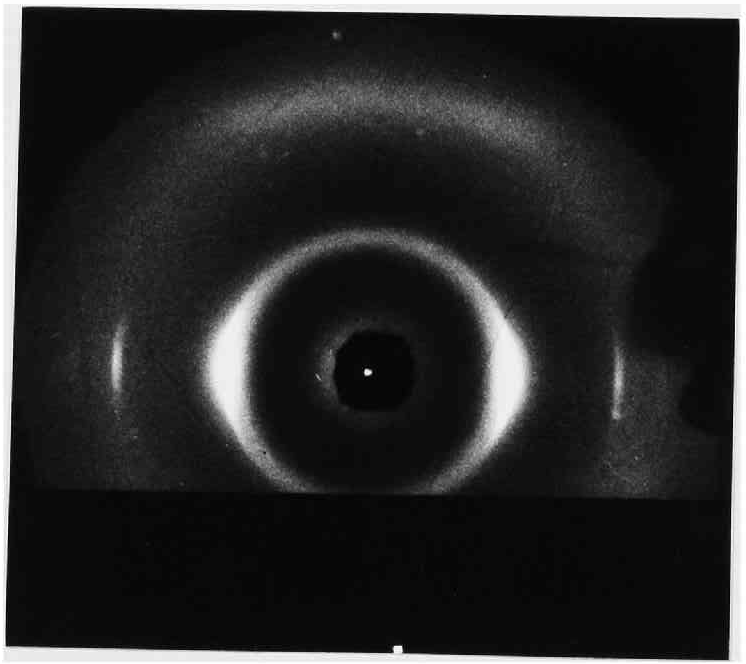

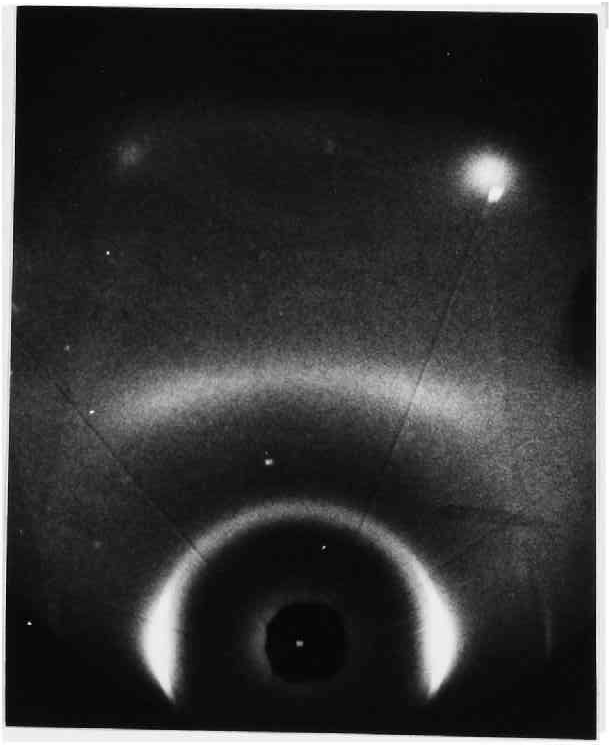

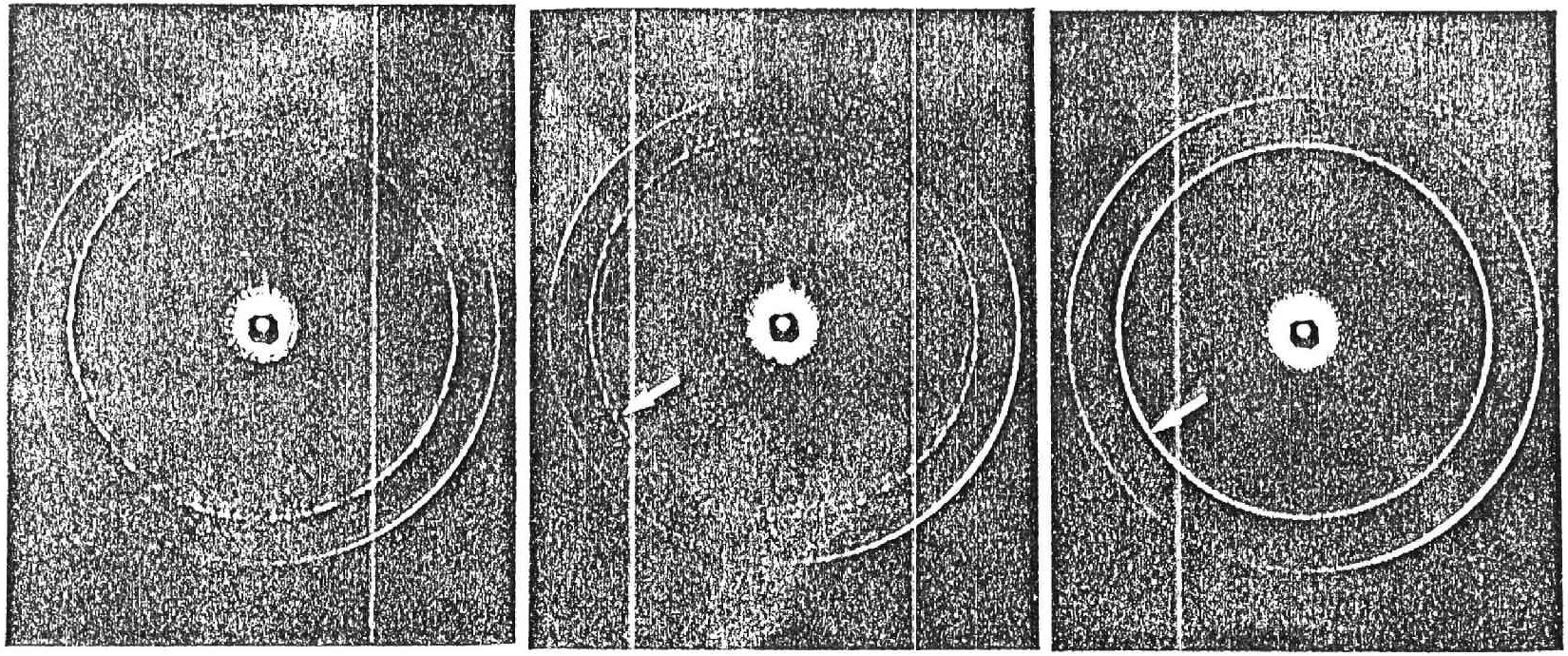

(a) (b) (c)

Fig 11